

Unveiling novel *Neocosmospora* species from Thai mangroves as potent biocontrol agents against *Colletotrichum* species

Anthikan Klomchit¹, Mark S. Calabon², Sompradtana Worabandit¹, Jack A. Weaver³, Elfina M. Karima⁴, Fabrizio Alberti³, Claudio Greco^{4,*}, Siraprapa Mahanil^{1,*}

¹School of Science, Mae Fah Luang University, Chiang Rai 57100, Thailand

²Division of Biological Sciences, College of Arts and Sciences, University of the Philippines Visayas, Miagao, Iloilo 5024, Philippines

³School of Life Sciences, University of Warwick, Gibbet Hill Road, Coventry CV4 7AL, United Kingdom

⁴Department of Biosciences, Swansea University, Swansea SA2 8PP, United Kingdom

*Corresponding authors. Department of Biosciences, Swansea University, Swansea, SA2 8PP, UK. E-mail: claudio.greco@swansea.ac.uk, and School of Science, Mae Fah Luang University, Chiang Rai, 57100, Thailand. E-mail: siraprapa.bro@mfu.ac.th

Abstract

Aims: *Neocosmospora* species are saprobes, endophytes, and pathogens belonging to the family *Nectriaceae*. This study aims to investigate the taxonomy, biosynthetic potential, and application of three newly isolated *Neocosmospora* species from mangrove habitats in the southern part of Thailand using phylogeny, bioactivity screening, genome sequencing, and bioinformatics analysis.

Methods and results: Detailed descriptions, illustrations, and a multi-locus phylogenetic tree with large subunit ribosomal DNA (LSU), internal transcribed spacer (ITS), translation elongation factor 1-alpha (*ef1-α*), and RNA polymerase II second largest subunit (*RPB2*) regions showing the placement of three fungal strains, MFLUCC 17–0253, MFLUCC 17–0257, and MFLUCC 17–0259 clustered within the *Neocosmospora* clade with strong statistical support. Fungal crude extracts of the new species *N. mangrovei* MFLUCC 17–0253 exhibited strong antifungal activity to control *Colletotrichum truncatum* CG-0064, while *N. ferruginea* MFLUCC 17–0259 exhibited only moderate antifungal activity toward *C. acutatum* CC-0036. Thus, *N. mangrovei* MFLUCC 17–0253 was sequenced by Oxford nanopore technology. The bioinformatics analysis revealed that 49.17 Mb genome of this fungus harbors 41 potential biosynthetic gene clusters.

Conclusion: Two fungal isolates of *Neocosmospora* and a new species of *N. mangrovei* were reported in this study. These fungal strains showed activity against pathogenic fungi causing anthracnose in chili. In addition, full genome sequencing and bioinformatics analysis of *N. mangrovei* MFLUCC 17–0253 were obtained.

Impact Statement

The novel fungus, *Neocosmospora mangrovei* MFLUCC 17–0253 displays promising potential for sustainable agriculture. Furthermore, bioinformatics analysis of the genome of this species revealed the potential for diverse compound production for applications in pharmaceutical, agrichemical, and food industries.

Keywords: one new taxon; bioactivity; mangrove fungi; multi-locus phylogenetic analyses; whole genome; biosynthetic gene clusters

Introduction

Neocosmospora, typified by *N. vasinfecta*, was first introduced by Smith (1899) as pathogenic fungi of wilt disease in cotton, watermelon, and cowpea. Generally, this genus can be characterized by superficial, solitary to gregarious, with globose to pyriform, multiseptate, subcylindrical macroconidia slightly curved with the tip cells slightly hooked. These macroconidia are thick-walled and contain ornamented ascospores without germ pores (Pfenning 1995, Rossman et al. 1999, Lombard et al. 2015). Although *Neocosmospora* is considered to be one of the major groups of plant pathogenic fungi, it is also recognized as a taxon of rich species diversity, which to a great extent remains understudied. Currently, the genus *Neocosmospora* comprises 129 morphological species and members of *Neocosmospora* are saprobes, endophytes, and pathogens in plant debris and living plant material (Hirooka et al. 2012, Lombard et al. 2015, Sandoval-Denis et al. 2019). The members of *Neocosmospora* are mainly docu-

mented from woody or herbaceous plants such as *Pistacia vera*, *Citrus sinensis*, *Camellia sinensis*, and *Morus alba*. This genus has a cosmopolitan distribution in tropical, subtropical, and temperate climate regions. Guarnaccia et al. (2018, 2021) reported that perhaps the perithecia are predominantly formed in tropical or subtropical regions. *Neocosmospora* has been used in several industrial applications, due to its ability to produce several enzymes such as chitosanases, cutinases, hydrolases, laccases, and lyases (Mannesse et al. 1995, Longhi et al. 2000, Liu and Bao 2009, Wu and Nian 2014, Jallouli et al. 2015). Species of this genus are also sources of cytotoxic compounds and secondary metabolites with antimicrobial activity (Nomila Merlin et al. 2013, Lee et al. 2014, Takemoto et al. 2014, Rathna et al. 2016, Chowdhury et al. 2017, Klomchit et al. 2021).

In this study, three fungal strains, MFLUCC 17–0253, MFLUCC 17–0257, and MFLUCC 17–0259, were isolated from mangrove habitats in the southern part of Thailand.

Received 22 December 2023; revised 29 February 2024; accepted 8 May 2024

© The Author(s) 2024. Published by Oxford University Press on behalf of Applied Microbiology International. This is an Open Access article distributed under the terms of the Creative Commons Attribution License (<https://creativecommons.org/licenses/by/4.0/>), which permits unrestricted reuse, distribution, and reproduction in any medium, provided the original work is properly cited.

Phylogenetic analyses of the combined large subunit ribosomal DNA (LSU), internal transcribed spacer (ITS), translation elongation factor 1- α (*ef1- α*), and RNA polymerase II second largest subunit (*RPB2*) regions were carried out. Morphological features and molecular data confirmed that MFLUCC 17-0253 and MFLUCC 17-0257 were new species of *Neocosmospora*, and MFLUCC 17-0259 is the known *N. ferruginea*. The distinctions between the new taxa and closely related taxa are discussed. We also include an evaluation of their antifungal activity against *Colletotrichum* spp., the causal agent that causes anthracnose disease in chili. Furthermore, the genome of *Neocosmospora mangrovei* MFLUCC 17-0253 was sequenced by Oxford nanopore technology and bioinformatics analysis was used to identify the biosynthetic potential of this strain. To the best of our knowledge, we are the first to publish the genome sequence of *N. mangrovei*.

Materials and methods

Morphological examinations

The fungal specimens were received from the Mae Fah Luang University Culture Collection (MFLUCC), Center of Excellence in Fungal Research, Chiang Rai, Thailand. These fungal strains were isolated from mangrove trees from Phetchaburi and Ranong provinces, Thailand, in 2016, as described in Norphanphoun et al. (2018). The fungal colonies were characterized using potato dextrose agar (PDA) and carnation leaf piece agar (CLA; Fisher 1982). Strains were incubated at 28°C with alternating periods of light and darkness (12 h/12 h). Colony growth rates were measured after one week on PDA. Sporulation was induced and observed from a three-week-old culture on CLA. Micromorphological characteristics, including size and shape of conidia, conidiogenous cells, and chlamydospores were determined from colonies grown on CLA using a Motic SMZ 168 Series dissection light microscope. Fungal fruiting bodies were documented using Nikon Eclipse 80i microscope-camera system. Measurements of microscopic characters were calculated using Tarosoft Image Frame Work program (IFW) version 0.97, and all photographic plates were made using Adobe Photoshop CS6 version 13.12.

DNA extraction, specific gene sequencing, and phylogenetic analysis

The genomic DNA extraction was performed from fresh mycelium scraped out of the colony surface of PDA using the PureDireX Genomic DNA Isolation Kit (Plant), according to the manufacturer's instructions (BIO-HELIX, Keelung City, Taiwan). Four primer pairs were used for PCR amplification, including LROR/LRS (LSU); Vilgalys and Hester (1990), ITS4/ITS5 (ITS region of the ribosomal RNA gene; White et al. 1990), EF1-728F/EF1-986 (translation elongation factor 1- α gene (*ef1- α*); Carbone and Kohn 1993), and *fRPB2-5F/RPB2-7R* (RNA polymerase II gene (*RPB2*); Liu et al. 1999). PCR purification and sequencing of amplified PCR products were carried out at Biogenomed Co., Ltd. using the primers mentioned above. The phylogenetic relationships between species were studied using a combined data set containing LSU, ITS (4/5), *ef1- α* , and *RPB2* sequences. Sequences were assembled using BioEdit and aligned with MAFFT v.7 on the online server (<https://mafft.cbrc.jp/alignment/server/>) (Kato and Standley 2013). Aligned sequences were automatically trimmed using TrimAl v.1.3 with the gappyout setting on

Table 1. Genome assembly statistics for *Neocosmospora* sp.

Parameter	<i>Neocosmospora mangrovei</i> MFLUCC 17-0253
Number of contigs	20
Total contigs length	49 172 478
Mean contig size	2 458 623.90
Contig size first quartile	875 593
Median contig size	2 579 391
Contig size third quartile	3 931 106
Longest contig	5 150 129
Shortest contig	63 679
Contigs > 100 K nt	20 (100%)
Contigs > 1 M nt	14 (70%)
N50	3 561 890
L50	6
N80	2 504 111
L80	11
Genes	15 294
Protein-coding genes	15 000
exons	41 487
CDSs	41 193
tRNAs	294

the web server (<http://phylemon.bioinfo.cipf.es/utilities.html> [accessed on 20 May 2022]). The online tool "ALTER" was used to convert the alignment file to phylip and nexus formats (Glez-Peña et al. 2010). Maximum likelihood analysis using RAxML and Bayesian inference (BI) analyses were done on the CIPRES Science Gateway platform (Miller et al. 2012). Parameters for maximum likelihood were set to rapid bootstrapping, and the analysis was carried out using 1000 replicates. Phylograms were visualized with FigTree v1.4.0 (available at <http://tree.bio.ed.ac.uk/software/figtree/>) and annotated in Microsoft PowerPoint (2010; Table 1).

Assessing the antifungal activity against anthracnose disease in chili

The pathogenic fungus that caused anthracnose disease in chili, *C. truncatum*, CG-0064 was kindly provided by Chia Tai Co., Ltd. (Bangkok, Thailand). A dual culture assay was used to screen the antifungal activity of the *N. mangrovei* MFLUCC 17-0253, *N. mangrovei* MFLUCC 17-0257, and *N. ferruginea* MFLUCC 17-0259 against the above-mentioned pathogen. Briefly, an 8-mm mycelium plug of growing saprobic fungi and pathogens was placed 3 cm apart on the PDA plate's surface and plates were incubated at 28°C. The PDA plate inoculated with only one pathogen was used as a control. After ten days of incubation, the radial growth of pathogenic fungi was recorded and converted into colony area (D) following the formula:

$$\text{Area of fungal colony} = \pi r^2. \quad (1)$$

The inhibition % of endophytic fungi to a pathogenic fungus was calculated using the formula:

$$\text{Inhibition (\%)} = \frac{D1 - D2}{D1} \times 100, \quad (2)$$

where D1 indicates the colony area of the pathogen in the control plate and D2 represents the colony area of the pathogen in the antagonistic assay.

For poisoned food assay and in planta assay, the fungal crude extract of *N. mangrovei* MFLUCC 17-0253 was obtained from the liquid-liquid chemical extraction method by

ethyl acetate (EtOAc) as previously described in Brooks et al. (2022). The poisoned food assay was performed by excising mycelial plugs (7 mm diameter) from cultures with actively growing pathogenic fungi and then placed in the center of PDA plates mixed with either fungal crude extract (final concentration at 0.6 and 0.9 mg/mL), sterile water, and fungicide (Captan with final concentration 0.6 mg/mL). After incubating the plate at 28°C for ten days, a digital caliper was used to measure pathogenic fungi radial (r) growth. The radial growth was recorded ten days post-incubation and converted into an area of colony (D). The inhibition percentage was calculated using formula 2.

For the planta assay, the *C. truncatum*, CG-0064, and *C. acutatum*, CC-0036 were separately cultured on V8 agar plates (200 mL V8® Campbell's, 20 g agar, 3 g CaCO₃) for 22 days to induce sporulation. Spores were washed off from the culture plate using sterile water with 20% (v/v) tween 20. Spore solutions were prepared and adjusted to 1 × 10⁶ spores/mL following the method described in Brooks et al. (2022). The 20 µL of the spore mixture with either fungal crude extract (final concentration 0.9, 2.7, and 5.4 mg/mL), sterile water (negative control), Captan (final concentration 0.6 mg/mL; positive control) were dropped on disinfected chili leaves. Inoculated leaves were placed in plastic containers with moist paper towels for five days. Leaves were cut and stained with Coomassie Brilliant Blue mixture following methods described in Brooks et al. (2022). A light microscope was used to observe hyphal coverage on the plant material. Inhibition of hyphal expansion was calculated using formula 2.

All experiments were performed in a completely randomized design (CRD) with three replications and the experiments were repeated three times. Statistical analyses were performed using Duncan's multiple range test (DMRT) and the SPSS V16.0 statistical package software program (SPSS Inc 2007).

Genome sequencing, assembly, and error correction

The genomic DNA of *N. mangrovei* sp. MFLUCC 17-0253 was prepared by DNeasy Plant Kits (Qiagen) and DNA library was prepared using kit SQK-LSK109 from Oxford Nanopore Technology (ONT). The manufacturer's protocol was modified for DNA repair and end prep stages by increasing the incubation time and temperature after ethanol washing to 15 minutes minimum at 37°C. Native barcode ligation took place at 37°C for 30 minutes. The long fragment buffer was used to enrich DNA fragments of 3 kb or longer. The 1.2 µg of genomic DNA was loaded at the beginning of library preparation. The library was sequenced on a MinION Mk1C (ONT) with a FLO-MIN-106 R9.4 flow cell (ONT). The raw data produced was base-called and demultiplexed using Guppy v6.0.1. Guppy used config file dna_r9.4.1_450bps_hac.cfg; all other parameters were left on default. Outputs were merged into a single.fastq file that was inputted into Flye version 2.9 using the nano-hq setting to assemble the draft genome (Kolmogorov et al. 2019). The draft genome was polished by aligning to the raw reads with Minimap2 v2.24 (Li 2018) and correcting errors using Racon v1.4.20 (Vaser et al. 2017), the values given to bases were as follows: 8 for matches, -6 for mismatches, and -8 for gaps, with a 500-base window size. The output from Racon was entered back into Minimap2 and the process repeated for four total rounds of polishing. Medaka v1.5.0 (ONT) was used to make further corrections

for the genome against model r941_min_high_g360. The polished genome was analyzed using BUSCO v5.0.0 against the sordariomycete odb10. Functional annotation was performed using the Funannotate version 1.8.9 pipeline (Palmer and Stajich 2020). The prediction and annotation of functional elements were done using the BUSCO Hypocreales database (*Neocosmospora* falls within the Hypocreales order), minimum training models were lowered to 100, and the Augustus optimization setting was called. Unless specified, all settings were left on their default parameters. CMScan (Burge et al. 2013) was used with StructRNAfinder (Arias-Carrasco et al. 2018) for screening for non-coding RNA, with the Rfam database (Griffiths-Jones et al. 2005) as the input.

Bioinformatics analysis

The genome of *N. mangrovei* MFLUCC 17-0253 was analyzed using antiSMASH fungal version 7.1.0; the detection strictness was set to "relaxed" and the extract features "KnownClusterBlast," "ClusterBlast," "SubClusterBlast," "MIBiG cluster comparison," "ActiveSiteFinder," "REFinder," and "Cluster Pfam analysis" were set on (Blin et al. 2023). The genes predicted in biosynthetic gene clusters (BGCs) were further searched using NCBI BLAST.

Results

Phylogenetic analyses

The combined LSU, ITS (4/5), *ef1-α*, and *RPB2* dataset comprised of 73 taxa from *Nectriaceae*, with *F. agapanthi* (NRRL 54463), *F. ananatum* (CBS 118516), *F. bulbicola* (CBS 220.76), *F. fujikuroi* (CBS 221.76), *F. torreyae* (CBS 133858), and *F. tricinctum* (CBS 393.93) as outgroup taxa (Table S1). The analyzed dataset, after trimming, comprised a total of 4337 characters, including gaps (LSU = 473 bp, ITS (4/5) = 1053 bp, *ef1-α* = 678 bp, and *RPB2* = 2133 bp) with 1514 distinct alignment patterns and 32.60% proportion of gaps and completely undetermined characters. The ML analysis for the combined dataset provided the best scoring tree (Fig. 1) with a final ML optimization likelihood value of 33795.848267 (ln). The BI was terminated when the average standard deviation of split frequencies at the end of total MCMC generations reached 0.009230. Phylogenetic analyses of the combined data matrix resulted in well-resolved clades (Fig. 1). The tree topologies resulting in ML and BI analyses were congruent.

In the phylogenetic analyses (Fig. 1), all *Neocosmospora* sequences clustered together with maximum statistical support. The two strains of *N. mangrovei* (MFLUCC 17-0253, MFLUCC 17-0257) were sister to *N. macrospora* (CPC 28192; CBS 142424; CPC 28193), while MFLUCC 17-0259 nested with strains of *N. ferruginea*.

Taxonomy

Neocosmospora mangrovei A. Klomchit, M.S. Calabon, C. Norphanphoun, and S. Brooks, sp. nov. (Fig. 2).

Mycobank number: MB 852465

Etymology: Named after the fungal habitat from mangrove habitat, where the fungus was isolated.

Holotype: MFLU 22-0153

Colonies reaching 40–55 mm diameter on PDA after 14 days at 24 °C, colony circular, white, flat, entire to filiform, velvety; reverse white to pale straw.

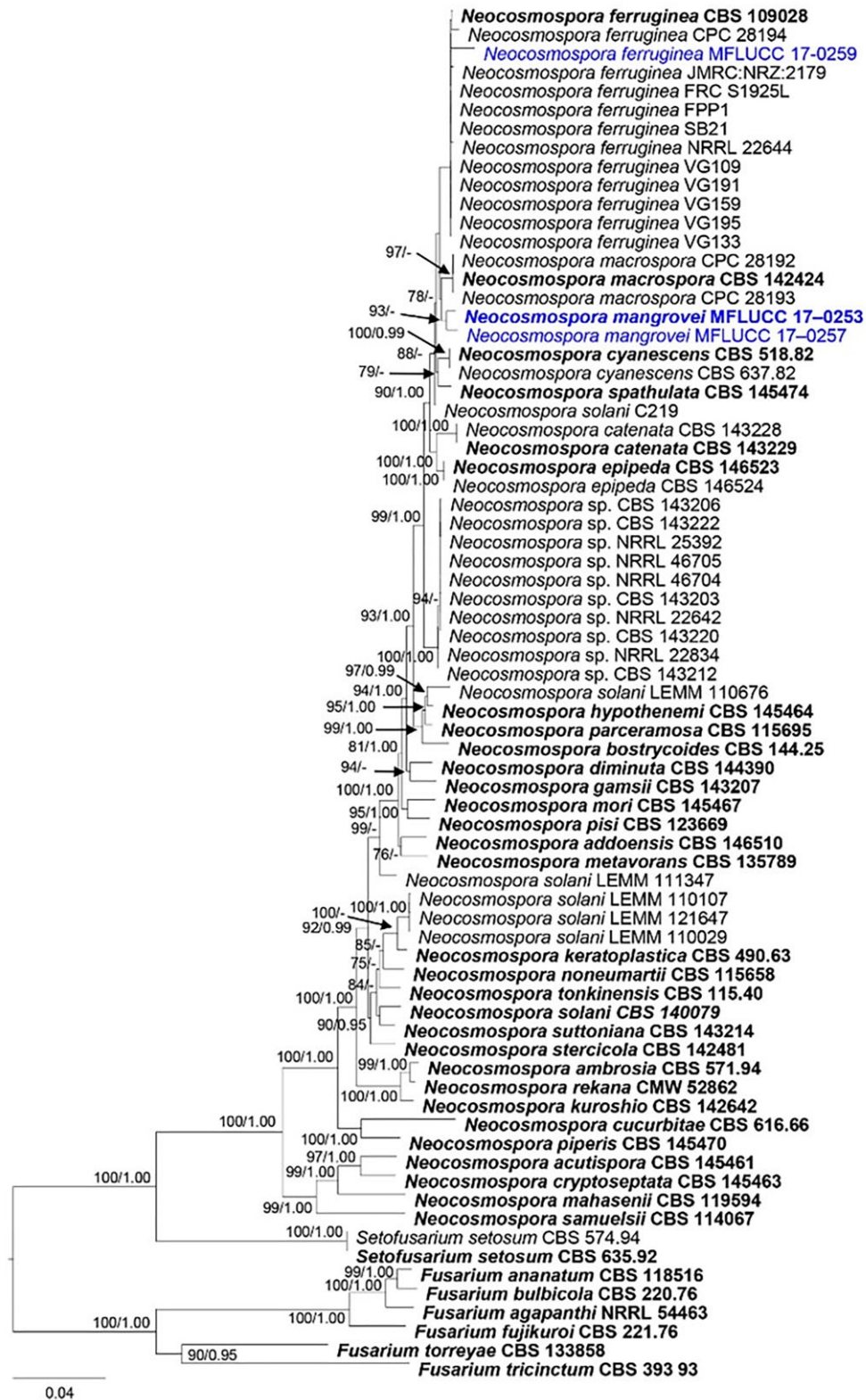


Figure 1. RAxML analysis of combined *ef1-α*, ITS, LSU, and *RPB2* sequence datasets comprised 73 strains of Noval strains, MFLUCC 17-0253, MFLUCC 17-0257, MFLUCC 17-0259, and *Nectriaceae* with six *Fusarium* species (*F. agapanthi* NRRL 54463, *F. ananatum* CBS 118516, *F. bulbicola* CBS 220.76, *F. fujikuroi* CBS 221.76, *F. torreyae* CBS 133858, and *F. tricinctum* CBS 393.93) as the outgroup taxa. Bootstrap support values for ML equal to or >70% and BYPP equal to or >0.95 are given above the nodes.

Conidiophores on aerial mycelium straight, smooth, and thin-walled, simple, terminal, single monophialides; *phialides* 36.5–74.0 × 2.5–5.5 μm (\bar{x} = 60.8 × 3.8 μm, n = 30), subulate to acicular, smooth and thin-walled, conidiogenous

loci with inconspicuous periclinal thickening and non-flared, minute collarettes; aerial conidia of two types: *microconidia* 4.5–8.0 × 1.5–3.5 μm (\bar{x} = 6.3 × 2.7 μm, n = 50), subglobose, mostly ellipsoidal, straight to slightly curved, often with a

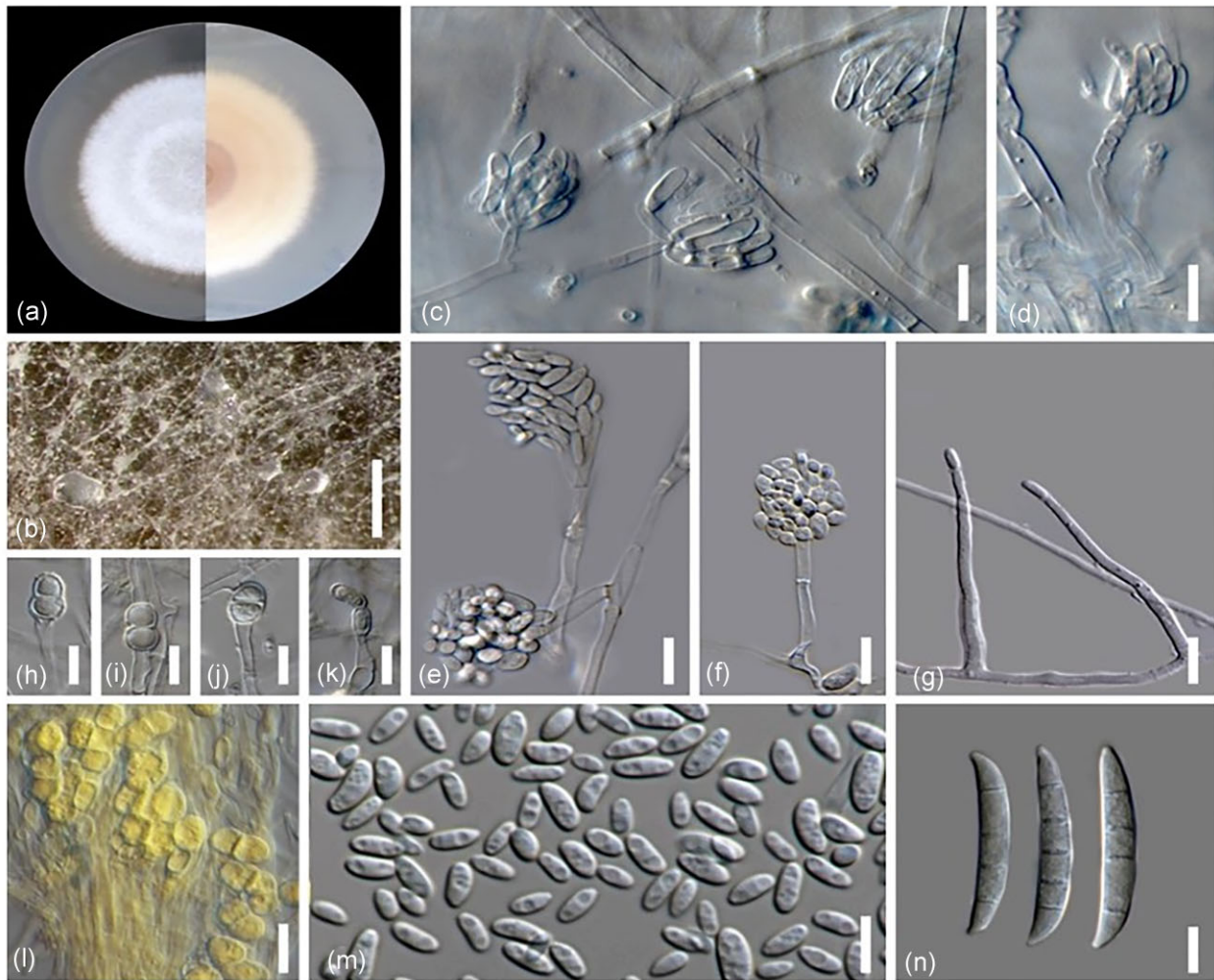


Figure 2. *Neocosmospora mangrovei* (MFLUCC 17–0253, ex-type culture). (a) Colonies on PDA (obverse and reverse); (b) mycelia on PDA with aerial conidiophores and mass of conidia; (c, d, e, f, g) aerial conidiophores; (h, i, j, k, l) chlamydospores; (m) aerial microconidia; (n) aerial macroconidia. Scale bars: (b) 500 µm; (c–n) 10 µm.

flattened base, aseptate, hyaline, smooth- and thin-walled, clustering in false heads at tip of monophialides; *macroconidia* 39–45 × 4.5–6.0 µm (\bar{x} = 42.8 × 5.2 µm, n = 10), falcate, straight to slightly dorsiventrally curved, apical cell blunt and slightly curved; basal cell inconspicuously to moderately notched, 4–5-septate, predominantly 4-septate, hyaline, smooth- and thick-walled. *Sporodochia* not observed. *Chlamydospores* 11–20 × 5–10 µm (\bar{x} = 15.6 × 7.4 µm, n = 50), abundantly formed, globose to subglobose, smooth- to verruculose and thick-walled, terminal or intercalary in hyphae or conidia, solitary or in chains.

Material examined: Thailand, Ranong Province, The Ranong Biosphere Reserve, on branches of *Rhizophora apiculata*, 7 December 2016, Chada Norphanphoun, NG27b (MFLU 22–0153, dried culture, holotype, permanently preserved in a metabolically inactive state), ex-type living culture MFLUCC 17–0253; on branches of *R. mucronata*, NG37b (MFLU 22–0154, dried culture, paratype, permanently preserved in a metabolically inactive state), ex-paratype living culture MFLUCC 17–0257.

GenBank accession numbers: MFLUCC 17–0253: LSU = ON833274, ITS = MT928792, *ef1-α* = OP272135;

MFLUCC 17–0257: LSU = ON833275, ITS = MT928793, *ef1-α* = OP272136, *RPB2* = OP272134.

Notes: Phylogenetic analyses of the combined sequence data (LSU, ITS, *ef1-α*, *RPB2*) showed that *N. mangrovei* is sister taxon to *N. macrospora*, and also belonged to the same subclade as *N. ferruginea*. Morphologically, *N. mangrovei* is distinct from *N. macrospora* by having longer phialides (36.5–74 × 2.5–5.5 µm vs. 19–67 × 2–5 µm) and larger chlamydospores (11–20 × 5–10 µm vs. 5–8.5 × 4.5–8 µm) (Sandoval-Denis et al. 2018). *Neocosmospora mangrovei* can be distinguished from *N. ferruginea* by the size of phialides [36.5–74 × 2.5–5.5 µm vs. (29.5–)31–40(–45) × 2.5–3.5 µm], microconidia [4.5–8 × 1.5–3.5 µm vs. (4–) 4.5–11(–20) × (15–) 2–4 (–6) µm], and chlamydospores (11–20 × 5–10 µm vs. 8–10 µm diameter) (Sandoval-Denis et al. 2019).

Neocosmospora ferruginea Sandoval-Denis et al., Persoonia 43: 130 (2019) (Fig. 3).

Mycobank number: MB831182

Colonies growing on PDA, reaching 40–55 mm diameter in 14 days at 24°C, colony circular, white, flat, entire, velvety to cottony, with or without white to straw concentric rings; reverse white to pale straw.

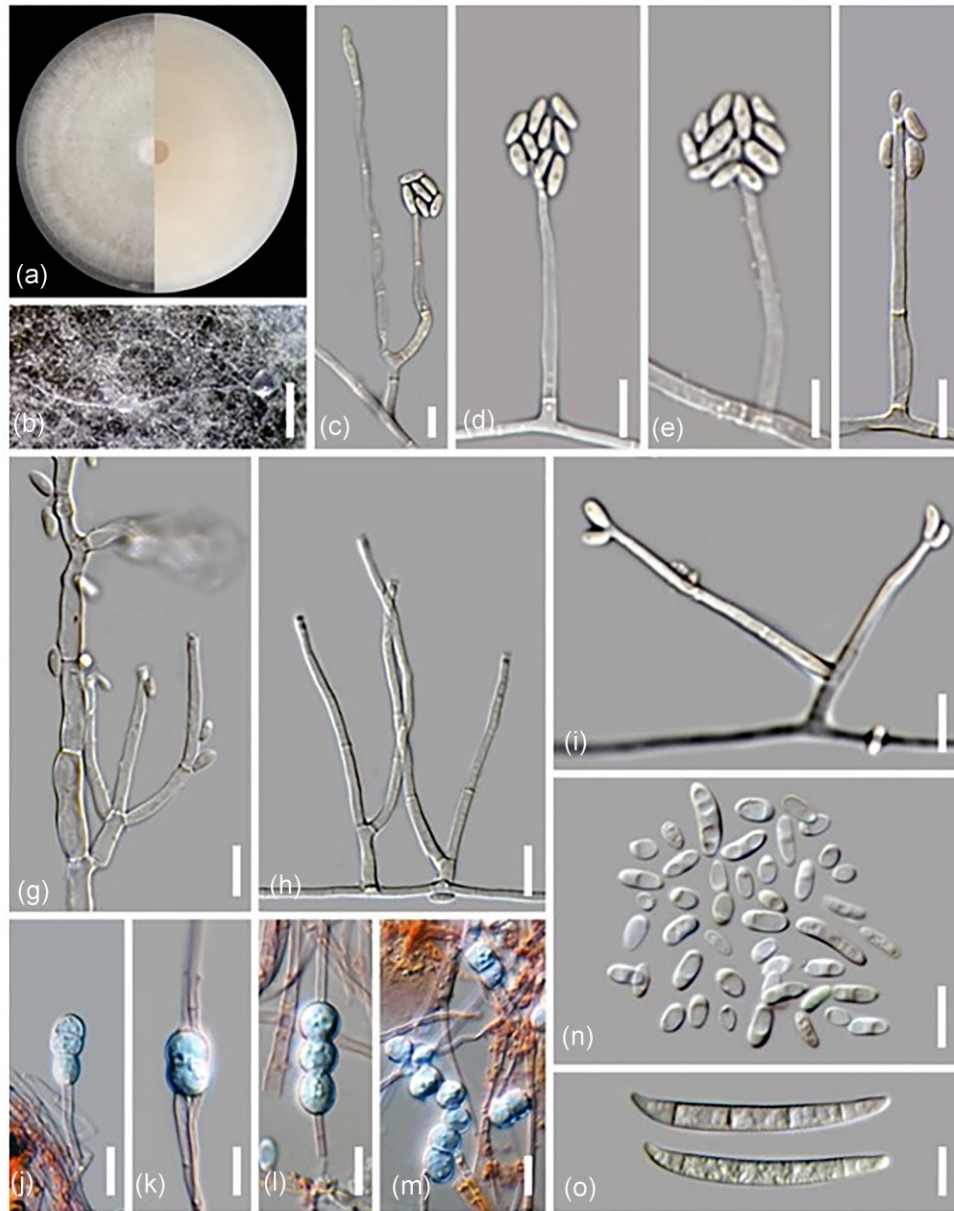


Figure 3. *Neocosmospora ferruginea* (MFLUCC 17-0259) (a) colonies on PDA (obverse and reverse); (b) mycelia on PDA with aerial conidiophores and mass of conidia; (c, d, e, f, g, h, i) aerial conidiophores; (j, k, l, m) chlamydospores; (n) aerial microconidia; (o) aerial macroconidia. Scale bars: (b) 500 µm; (c-o) 10 µm.

Conidiophores on aerial mycelium straight, smooth, and thin-walled, simple or branched several times verticillately, bearing terminal or lateral, single monophialides; phialides $35\text{--}73 \times 2.2\text{--}4.5 \mu\text{m}$ ($\bar{x} = 52.5 \times 3 \mu\text{m}$, $n = 50$) subulate, subcylindrical, to acicular, smooth- and thin-walled, conidiogenous loci with inconspicuous periclinal thickening and non-flared, minute collarettes; aerial conidia of two types: *microconidia* $6.60\text{--}14.5 \times 2.7\text{--}5.5 \mu\text{m}$ ($\bar{x} = 10.4 \times 4.1 \mu\text{m}$, $n = 50$) oval, obovoidal to ellipsoidal, mostly straight to slightly curved, often with a flattened base, aseptate, hyaline, smooth- and thin-walled, clustering in false heads at tip of monophialides; *macroconidia* up to $55 \mu\text{m}$, falcate, rarely straight with moderately curved ends, tapering toward base, septation sometimes indistinct or with thin transverse septa; apical cell of equal length or slightly longer than adjacent cell,

blunt to slightly hooked with rounded apex; basal cell inconspicuously to moderately notched, 4-septate, hyaline, smooth- and thick-walled. *Sporodochia* not observed. *Chlamydospores* $9\text{--}21.5 \times 5.5\text{--}10 \mu\text{m}$ ($\bar{x} = 13.7 \times 7/7 \mu\text{m}$, $n = 30$) abundantly formed, globose to subglobose, smooth- to verruculose and thick-walled, terminal or intercalary in hyphae or conidia, solitary, in chains or in clusters.

Material examined: Thailand, Ranong Province, The Ranong Biosphere Reserve, on branches of *Cerriops decandra*, 6 December 2016, Chada Norphanphoun, NG03b (MFLU 22-0152, dried culture, holotype, permanently preserved in a metabolically inactive state), living culture MFLUCC 17-0259.

GenBank accession numbers: LSU = ON833276, ITS = MT928794, *ef1- α* = OP272137.

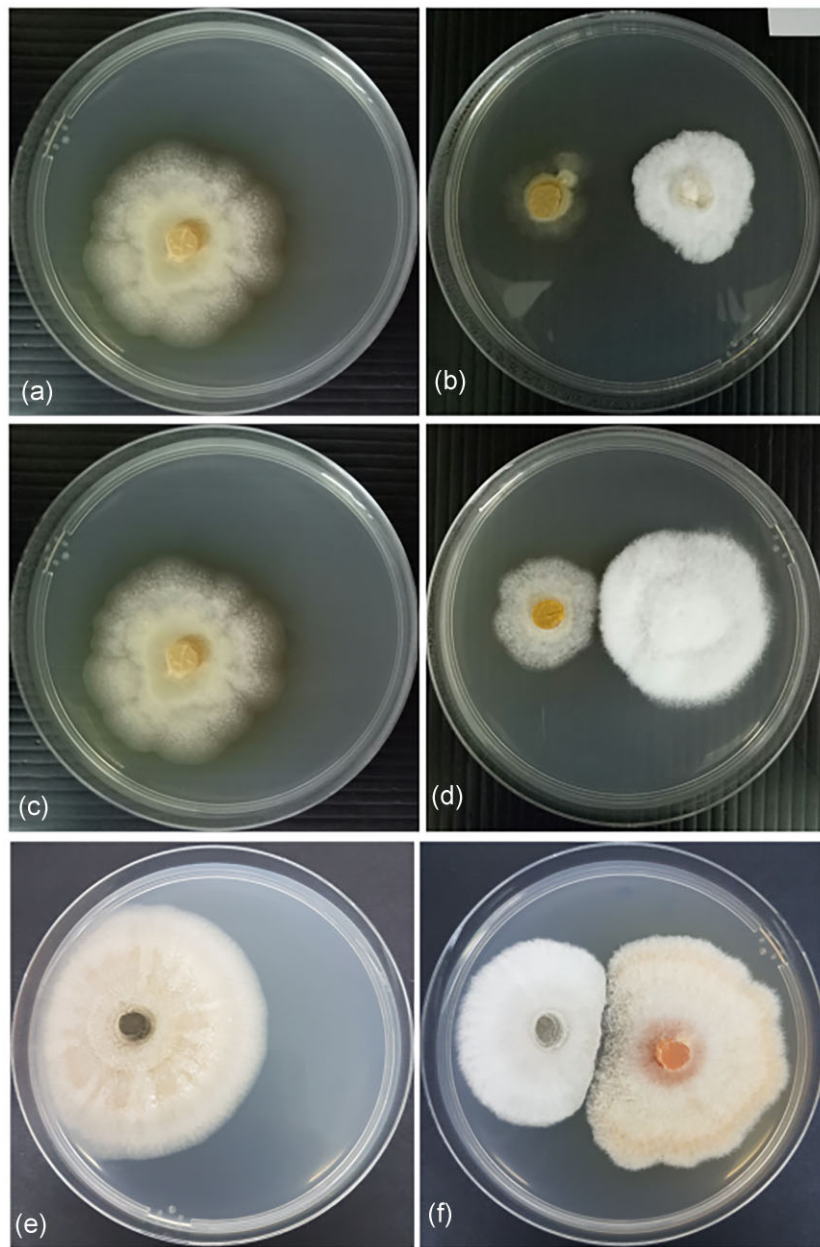


Figure 4. Dual culture assay between *C. truncatum* CG-0064 with *N. mangrovei* MFLUCC 17-0253 and *N. mangrovei* MFLUCC 17-0257 (a–d) and *C. acutatum* CC-0036 with *N. ferruginea* MFLUCC 17-0259 (e–f), *C. truncatum* CG-0064 (control; a, c), *N. mangrovei* MFLUCC 17-0253 and *C. truncatum* CG-0064 (b), *N. mangrovei* MFLUCC 17-0257 and *C. truncatum* CG-0064 (d), *C. acutatum* CC-0036 (control; e) *C. acutatum* CC-0036 with *N. ferruginea* MFLUCC 17-0259 (f).

Notes: In the multi-locus phylogenetic analysis shows that *N. ferruginea* MFLUCC 17-0259 clustered with strains of *N. ferruginea*. When compared with the holotype, *N. ferruginea* CBS 109028, *N. ferruginea* MFLUCC 17-0259 can be distinguished from by the size of phialides [$35\text{--}73 \times 2.2\text{--}4.5 \mu\text{m}$ vs. $(29.5\text{--})31\text{--}40(-45) \times 2.5\text{--}3.5 \mu\text{m}$], conidia [$6.6\text{--}14.5 \times 2.7\text{--}5.5 \mu\text{m}$ vs. $(4\text{--})4.5\text{--}11(-20) \times (1.5\text{--})2\text{--}4(-60 \mu\text{m})$], and chlamydoconidia ($9\text{--}21.5 \times 5.5\text{--}10 \mu\text{m}$ vs. $8\text{--}10 \mu\text{m}$ diameter) (Sandoval-Denis et al. 2019). *Neocosmospora ferruginea* MFLUCC 17-0259 shared the same subclade with *N. mangrovei* and *N. macrospora*. Morphologically, *N. ferruginea* MFLUCC 17-0259 has a larger microconidium ($6.6\text{--}14.5 \times 2.7\text{--}5.5 \mu\text{m}$ vs. $4.5\text{--}8 \times 1.5\text{--}3.5 \mu\text{m}$) than *N. mangrovei*. *Neocosmospora ferruginea* MFLUCC 17-0259 has

longer phialides ($35\text{--}73 \times 2.2\text{--}4.5 \mu\text{m}$ vs. $19\text{--}67 \times 2\text{--}5 \mu\text{m}$) and larger chlamydoconidia ($9\text{--}21.5 \times 5.5\text{--}10 \mu\text{m}$ vs. $5\text{--}8.5 \times 4.5\text{--}8 \mu\text{m}$) compared to *N. macrospora* (Sandoval-Denis et al. 2018).

Antagonistic activity against anthracnose disease

In the dual culture assay, *N. mangrovei* MFLUCC 17-0253 and *N. mangrovei* MFLUCC 17-0257 exhibited antagonistic effects against *C. truncatum*, CG-0064 resulting in mycelium growth inhibition percentages of $63.17\% \pm 4.15\%$ and $21.25\% \pm 6.22\%$, respectively (Fig. 4). The *N. ferruginea* MFLUCC 17-0259 exhibited $46.5\% \pm 7.47\%$ mycelium growth inhibition against *C. acutatum*, CC-0036 (Fig. 4).

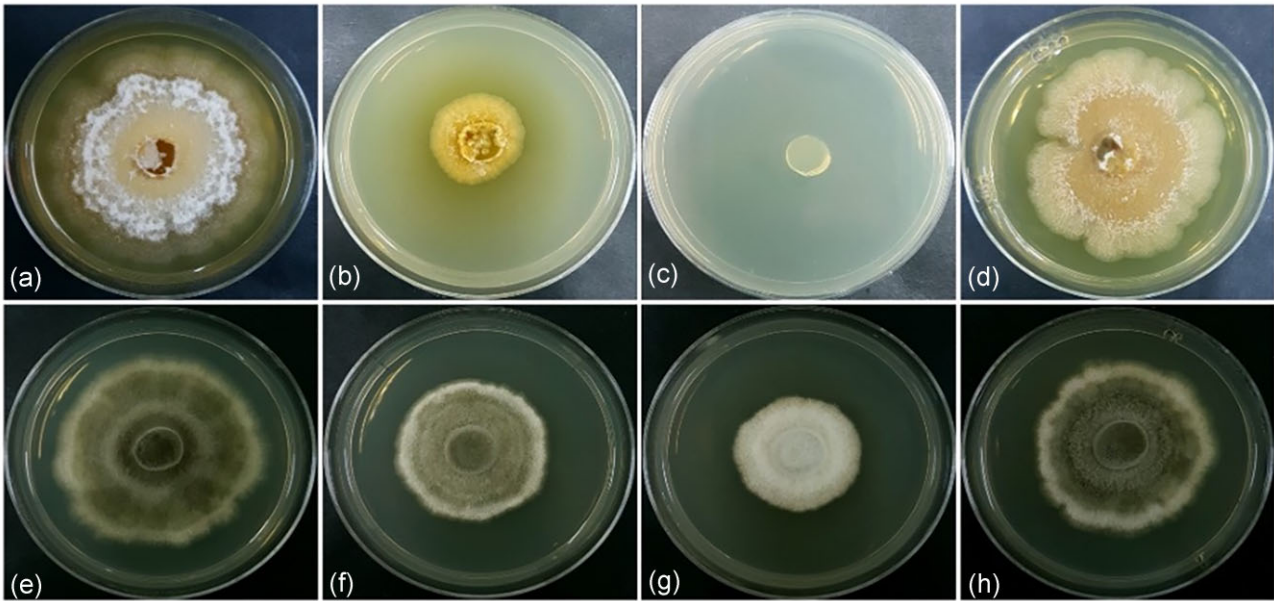


Figure 5. Growth of *C. truncatum* CG-0064 in poisoned food assay (a–d) grown on PDA at 28 °C after seven days, mixed with either sterile water (a), crude extract of *N. mangrovei* MFLUCC 17–0253 (0.6 mg/mL) (b), crude extract of *N. mangrovei* MFLUCC 17–0253 (0.9 mg/mL) (c), or captan (0.6 mg/mL) (d). Growth of *C. acutatum* CC-0036 in poisoned food assay (e–h) grown on PDA at 28 °C after 7 days, mixed with either sterile water (e), crude extract of *N. ferruginea* MFLUCC 17–0259 (0.6 mg/mL) (f), crude extract of *N. ferruginea* MFLUCC 17–0259 (0.9 mg/mL) (g), captan concentration (h).

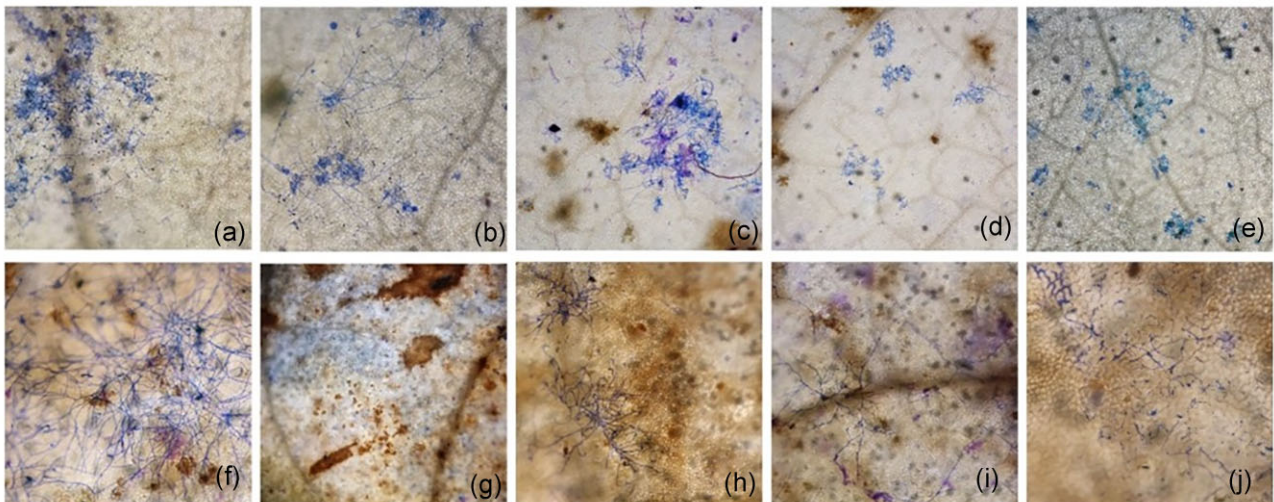


Figure 6. Hypha growth of *C. truncatum* CG-0064 (a–e) on chili leaves, spore solution mixed with either sterile water (a), captan (0.6 mg/mL) (b), crude extract of *N. mangrovei* MFLUCC 17–0253 (0.9 mg/mL); c), crude extract of *N. mangrovei* MFLUCC 17–0253 (2.7 mg/mL); d), or crude extract of *N. mangrovei* MFLUCC 17–0253 (5.4 mg/mL); e) at 5 days after incubation. Hypha growth of *C. acutatum* CC-0036 (f–j) on chili leaves, spore solution mixed with either sterile water (f), captan (g), crude extract of *N. ferruginea* MFLUCC-0259 (0.9 mg/mL); h), crude extract of *N. ferruginea* MFLUCC-0259 (2.7 mg/mL); i), or crude extract of *N. ferruginea* MFLUCC-0259 (2.7 mg/mL); j) at 5 days after incubation.

The dual assay displayed high antagonistic effects of *N. mangrovei* MFLUCC 17–0253 and *N. ferruginea* MFLUCC 17–0259 against *C. truncatum*, CG-0064, and *C. acutatum*, CC-0036, respectively. Thus, these two strains were further analyzed for antagonistic potential through poisoned food and in planta assays. Both assays confirmed the potency of fungal crude extract obtained from *N. mangrovei* MFLUCC 17–0253 toward *C. truncatum*, CG-0064. The fungal crude extract derived from *N. mangrovei* MFLUCC 17–0253 completely inhibited the growth of *C. truncatum*, CG-0064 in poisoned food (at a concentration of 0.9 mg/mL), and in planta assay (at a concentration of 2.7 mg/mL) (Fig. 5). At the

same time, fungal crude extract obtained from *N. ferruginea* MFLUCC 17–0259 displayed antagonistic effects against *C. acutatum*, CC-0036. At a concentration of 5.4 mg/mL, this fungal crude extract inhibited hyphal growth on chili leaves as high as 96.42% (Fig. 6; Table 2).

Genome sequencing for *N. mangrovei* MFLUCC 17-0253

Genomic DNA from new fungal species *N. mangrovei* MFLUCC 17–0253 was sequenced through Oxford nanopore sequencing. This led to ~2,507,796,378 bases from the

Table 2. Inhibition of *C. truncatum*, CG-0064 by *N. mangrovei* MFLUCC 17–0253 (A) and *C. acutatum*, CC-0036 by *N. ferruginea* MFLUCC 17–0259 (B) in poisoned food assay and in planta assays.

Treatments	Inhibition of mycelium growth (%) ¹	
	A	B
Poisoned food assay*		
0.6 mg/mL	82.64 ± 0.74b	53.67 ± 3.09b
0.9 mg/mL	100.00 ± 0.00a	69.39 ± 2.42a
Captan (0.6 mg/mL)	78.56 ± 20.79c	77.34 ± 3.00c
In planta assay		
0.9 mg/mL	68.75 ± 8.33	74.99 ± 11.66
2.7 mg/mL	100.00 ± 0.00	78.57 ± 10.00
5.4 mg/mL	100.00 ± 0.00	96.42 ± 4.65
Captan (0.6 mg/mL)	75.00 ± 1.09	100.00 ± 0.00

*Significant at $P = 0.05$.

¹Data are presented as mean ± S.D. values of three independent experiments.

nanopore data. As our assembly of *N. mangrovei* MFLUCC 17–0253 has a 49.17 Mb genome, this gives a 51x coverage. Assembly statistics reported in Table 1 show that this assembly has 20 contigs of significant size, some of these are likely to be assembled at the chromosomal level, although this requires further investigation to be determined. BUSCO (Manni et al. 2021) was used to determine the quality of the genomes by quantifying the completeness of core conserved genes in *N. mangrovei* MFLUCC 17–0253 that would be expected across the Hypocreales order. Supplementary Table S1 shows the conserved genes identified across the scaffold of this assembly, while Supplementary Table S2 shows the conserved proteins identified in the predicted proteome for this species.

Genome analysis

The predicted proteome generated using the Funannotate package was run through Eggno-mapper v2.1.7, through which 77.5% of the 15 000 protein-coding genes were able to be assigned a COG (Clusters of Orthologous Groups) functional category. The distribution of genes across these categories is shown in Supplementary Fig. S1. It is important to note that some genes are assigned multiple COG categories. Supplementary Fig. S2 shows that Eggno-mapper was also capable of assigning gene ontology terms, frequently with multiple terms assigned to individual predicted proteins, enzyme commission numbers, matches across multiple KEGG databases, and BRITe hierarchies are also included. A small number of predicted proteins (1.5%) could be assigned to matches in the CAZy database for carbohydrate-active enzymes, 1% were found to match with BiGG IDs. 76.3% of genes were matched to the Pfam database.

Biosynthetic gene clusters prediction

The genome of *N. mangrovei* MFLUCC 17–0253 was analyzed using antiSMASH fungal version 7.1.0. This analysis revealed a total of 41 putative BGCs, including 13 polyketide synthase (PKS), ten non-ribosomal peptide synthetase (NRPS), six NRPS-like BGCs, five terpenes, two ribosomally synthesized and post-translationally modified peptides (RiPPs), along with hybrid PKS-NRPS, indole, betalactone, phosphonate, and isocyanide (Fig. 7a). Out of 41 predicted BGCs, only six exhibited significant homolo-

gies to characterized BGCs. One polyketide containing BGC closely matches BGCs that have been linked to the biosynthesis of phenalenone precursors 1–2 and duclauxin 3 (Supplementary Fig. S3), while another polyketide BGC shows a high similarity to oxyjanvanicin 4 BGC (Supplementary Fig. S4). This BGC could be responsible for the biosynthesis of secondary metabolites previously isolated from this fungus, which are 2-methoxy-6-methyl-7-acetyl-8-hydroxy-1,4-naphthalenedione 5, 5,8-dihydroxy-7-acetyl-1,4-naphthalenedione 6, anhydrojavanicin 7, and fusarnaphthoquinones B 8 (Fig. 7c) (Klomchit et al. 2021). Additionally, one NRPS containing BGC was highly homologous to the BGC responsible for the biosynthesis of dimerumic acid 9 and metachelin A 10 (Supplementary Fig. S5). Furthermore, two NRPS BGCs displayed significant similarity to the BGCs of choline 11 (Supplementary Fig. S6) and sansalvamide 12 (Supplementary Fig. S7), respectively. Lastly, one hybrid NRPS-PKS BGC had high homology to the lucilactaene 13 BGC (Supplementary Fig. S8).

Discussion

Both *Fusarium* and *Neocosmospora* share similar features, including macroconidia; thus, there are different hypotheses as to the taxonomic and phylogenetic distinction between the *Neocosmospora* and the *F. solani* species complex (FSSC) (O'Donnell 2000). Geiser et al. (2013) recognized the *Fusarium* link broadly and considered *Neocosmospora* in the same group as *F. solani*. The same broad concept of *Fusarium* was present in O'Donnell et al. (2020) and Geiser et al. (2021). However, findings supported by Zeng and Zhuang (2017), Sandoval-Denis et al. (2018), and Crous et al. (2021) have justified the presence of a distinct genus representing a morphologically aberrant lineage within other groups, including *Neocosmospora* in FSSC. This study identified *Neocosmospora* species from the southern part of Thailand based on morphological and molecular data. The phylogenetic analysis of combined LSU, ITS, *ef1- α* , and *RPB2* regions of 73 additional taxa of *Neocosmospora* together with morphology confirmed the placement of new species within the genus. Two strains of *N. mangrovei* (MFLUCC 17–0253, MFLUCC 17–0257) sp. nov. are phylogenetically related to *N. macrospora* (Fig. 1, see Notes for morphological differences).

Previously, *N. mangrovei* MFLUCC 17–0253 has showcased its significance as a valuable source of beneficial secondary metabolite compounds. The identification of secondary metabolites, including mixture of 2-methoxy-6-methyl-7-acetyl-8-hydroxy-1,4-naphthalenedione 5, 5,8-dihydroxy-7-acetyl-1,4-naphthalenedione 6, anhydrojavanicin 7, and fusarnaphthoquinones B 8 from *N. mangrovei* MFLUCC 17–0253 has emerged as crucial for the cucurbit industry due to their antibacterial activity against the pathogenic bacterium, *Acidovorax citrulli* JT-003 (Klomchit et al. 2021). In this study, bioinformatics analysis identified a putative polyketide containing BGC that could be responsible for the biosynthesis of the metabolites. Furthermore, the current study highlighted the potent antifungal activity of *N. mangrovei* MFLUCC 17–0253 against pathogenic fungi causing anthracnose in chili. The promising efficacy of the novel *N. mangrovei* MFLUCC 17–0253 against two major plant diseases in crop production, combined with the identification of 41 putative BGCs in this study, suggests the potential for these BGCs to generate secondary metabolites

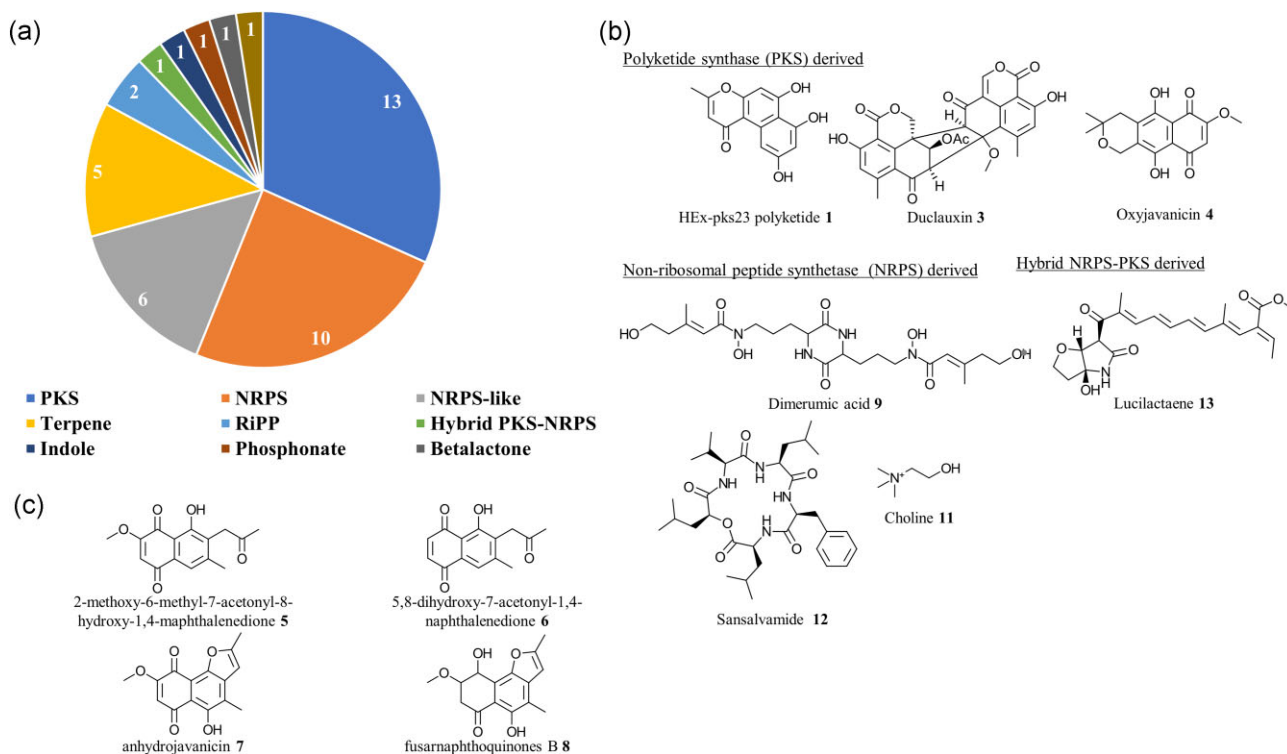


Figure 7. The biosynthetic potential of *N. mangrovei* MFLUCC 17–0253. (a) The distribution of the BGCs by type of natural products. Polyketide synthase (PKS), non-ribosomal peptide synthetase (NRPS), ribosomally synthesized and post-translationally modified peptides (RiPPs) (b) The structure of secondary metabolites that could be produced by this strain based on BGCs similarity to known BGCs in the literature. (c) Secondary metabolites previously isolated from *N. mangrovei* MFLUCC 17–0253.

that might effectively combat other plant diseases, thus making a significant discovery.

The *N. mangrovei* MFLUCC 17–0253 holds promise as a potential microbial biocontrol agent for future application in sustainable agriculture, as discussed above. This strain also shows promise to be a valuable resource for pharmaceutical applications. Six of the BGCs from this strain show high homology to BGCs that have been characterized to produce several secondary metabolites, including phenalenone, duclauxin, oxyjanvanicin, dimeric acid, metachelins, choline, sansalvamide, and lucilactaene. Notably, phenalenone, an aromatic polyketide, has been documented for its diverse bioactivities, including cytotoxic, antimicrobial, antioxidant, and anti-HIV properties (Harvey *et al.* 2018, Ibrahim *et al.* 2022). While oxyjanvanicin was reported to have antibacterial properties (Arnstein *et al.* 1946, Studt *et al.* 2012). Choline has a pivotal role in cell-membrane signaling (Hai *et al.* 2019). Moreover, other predicted compounds, including duclauxin, sansalvamide, and lucilactaene have efficacy against cancer cells, which are tumor cell lines, cancer HT-29, and p53-transfected cancer cells, respectively (Shahid *et al.* 2021, Styers *et al.* 2006, Kato *et al.* 2020).

The genome of *N. mangrovei* MFLUCC 17–0253 was sequenced using Oxford nanopore technology, which resulted in a very high-quality genome assembly, which highlights the advancement of this sequencing technology and its application for sequencing fungal genomes (Tamizi *et al.* 2022). More importantly, the genome of this species displays the potential for diverse compound production that is effective against significant plant diseases, and some with the possibility of pharmaceutical applications. Therefore, it is important to further

explore new species in this complex genus and assess their capabilities for both sustainable agriculture and pharmaceutical advancements.

Acknowledgements

The authors would like to acknowledge Dr. Chada Norphaphoun for fungal isolation and Asst. Prof. Dr. Putarack Chomnunti for her advice on phylogenetic tree analysis.

Supplementary data

Supplementary data is available at *JAMBIO Journal* online.

Conflict of interest: The authors declare that research was conducted in the absence of any commercial or financial relationships that could be construed as a potential conflict of interest.

Funding

C. Greco was supported by the BBSRC (BB/V005723/2). E. Karima's PhD Scholarship was supported by EPSRC/Swansea University (EP/W524694/1). Jack Weaver was supported by a scholarship from the Engineering and Physical Sciences Research Council and the Biotechnology and Biological Sciences Research Council [EP/L016494/1] through the Centre for Doctoral Training in Synthetic Biology (SynBioCDT). Fabrizio Alberti was supported by a UKRI Future Leaders Fellowship [MR/V022334/1]. Siraprapa Mahanil was supported by Mae Fah Luang University under the grant name "Reinventing University 2021."

Author contributions

Anthikan Klomchit (Data curation, Formal analysis, Investigation, Methodology, Software, Validation, Visualization, Writing – original draft, Writing – review & editing), Mark Seasat Calabon (Formal analysis, Investigation, Methodology, Writing – original draft), Sompradtana Worabandit (Investigation, Methodology, Software), Jack A. Weaver (Data curation, Formal analysis, Investigation, Methodology, Software, Validation, Writing – original draft, Writing – review & editing), Elfina M. Karima (Data curation, Formal analysis, Visualization, Writing – original draft), Fabrizio Alberti (Funding acquisition, Investigation, Project administration, Resources, Supervision, Writing – review & editing), Claudio Greco (Conceptualization, Data curation, Formal analysis, Funding acquisition, Investigation, Methodology, Project administration, Resources, Software, Supervision, Validation, Visualization, Writing – original draft, Writing – review & editing), and Siraprapa Mahanil (Conceptualization, Data curation, Formal analysis, Funding acquisition, Investigation, Methodology, Project administration, Resources, Software, Supervision, Validation, Visualization, Writing – original draft, Writing – review & editing)

Data availability

The genome sequences generated for this study were submitted to GenBank. BioSample metadata is publicly available in the NCBI database (<http://www.ncbi.nlm.nih.gov/biosample/>) under the Bioproject accession number PRJNA1053611.

References

- Arias-Carrasco R, Vásquez-Morán Y, Nakaya HI *et al.* StructRNAfinder: an automated pipeline and web server for RNA families prediction. *BMC Bioinf* 2018;19:1–7. <https://doi.org/10.1186/s12859-018-2052-2>.
- Arnstein HRV, Cook AH, Lacey MS. An antibacterial pigment from *Fusarium javanicum*. *Nature* 1946;157:333–4. <https://doi.org/10.1038/157333b0>.
- Blin K, Shaw S, Augustijn HE *et al.* antiSMASH 7.0: new and improved predictions for detection, regulation, chemical structures and visualisation. *Nucleic Acids Res* 2023;51:344.
- Brooks S, Klomchit A, Chimthai S *et al.* *Xylaria feejeensis*, SRNE2BP a fungal endophyte with biocontrol properties to control early blight and fusarium wilt disease in tomato and plant growth promotion activity. *Curr Microbiol* 2022;79:108. <https://doi.org/10.1007/s00284-022-02803-x>.
- Burge SW, Daub J, Eberhardt R *et al.* Rfam 11.0: 10 years of RNA families. *Nucleic Acids Res* 2013;41:226–32. <https://doi.org/10.1093/nar/gks1005>.
- Carbone I, Kohn LM. Ribosomal DNA sequence divergence within *Internal Transcribed Spacer 1* of the *Sclerotiniaceae*. *Mycologia* 1993;85:415–27. <https://doi.org/10.2307/3760703>.
- Chowdhury NS, Sohrab MH, Rana MS *et al.* Cytotoxic Naphthoquinone and Azaanthraquinone derivatives from an endophytic *Fusarium solani*. *J Nat Prod* 2017;80:1173–77. <https://doi.org/10.1021/acs.jnatprod.6b00610>.
- Crous PW, Lombard L, Sandoval-Denis M *et al.* *Fusarium*: more than a node or a foot-shaped basal cell. *Stud Mycol* 2021;98:100116. <https://doi.org/10.1016/j.simyco.2021.100116>.
- Fisher NL. Carnation leaves as a substrate and for preserving cultures of *Fusarium* species. *Phytopathology* 1982;72:151–53. <https://doi.org/10.1094/Phyto-72-151>.
- Geiser DM, Al-Hatmi AMS, Aoki T *et al.* Phylogenomic analysis of a 55.1-kb 19-gene dataset resolves a monophyletic *Fusarium* that includes the *Fusarium solani* species complex. *Phytopathology* 2021;111:1064–79. <https://doi.org/10.1094/PHYTO-08-20-0330-LE>.
- Geiser DM, Aoki T, Bacon CW *et al.* One fungus, one name: defining the genus *Fusarium* in a scientifically robust way that preserves long-standing use. *Phytopathology* 2013;103:400–8. <https://doi.org/10.1094/PHYTO-07-12-0150-LE>.
- Glez-Peña D, Gómez-Blanco D, Reboiro-Jato M *et al.* ALTER: program-oriented conversion of DNA and protein alignments. *Nucleic Acids Res* 2010;38:W14–8. <https://doi.org/10.1093/nar/gkq321>.
- Griffiths-Jones S, Moxon S, Marshall M *et al.* Rfam: annotating non-coding RNAs in complete genomes. *Nucleic Acids Res* 2005;33:121–4. <https://doi.org/10.1093/nar/gki081>.
- Guarnaccia V, Sandoval-Denis M, Aiello D *et al.* *Neocosmospora perseae* sp. nov., causing trunk cankers on avocado in Italy. *Fungal Syst Evol* 2018;1:131–40. <https://doi.org/10.3114/fuse.2018.01.06>.
- Guarnaccia V, Van Niekerk J, Crous PW *et al.* *Neocosmospora* spp. associated with dry root rot of citrus in South Africa. *Phytopathol Mediterr* 2021;60:79–100. <https://doi.org/10.36253/phyto-12183>.
- Hai Y, Huang AM, Tang Y. Structure-guided function discovery of an NRPS-like glycine betaine reductase for choline biosynthesis in fungi. *Proc Natl Acad Sci* 2019;116:10348–53. <https://doi.org/10.1073/pnas.1903282116>.
- Harvey CJB, Tang M, Schlecht U *et al.* HEX: a heterologous expression platform for the discovery of fungal natural products. *Sci Adv* 2018;4:5459. <https://doi.org/10.1126/sciadv.aar5459>.
- Hirooka Y, Rossman AY, Samuels GJ *et al.* A monograph of *Al-lantonectria*, *Nectria*, and *Pleonectria* (*Nectriaceae*, *Hypocreales*, *Ascomycota*) and their pycnidial, sporodochial, and synnematosus anamorphs. *Stud Mycol* 2012;71:1–210. <https://doi.org/10.3114/sim0001>.
- Ibrahim SRM, Omar AM, Muhammad YA *et al.* Advances in fungal phenaloenones-natural metabolites with great promise: biosynthesis, bioactivities, and an in silico evaluation of their potential as human glucose transporter 1 inhibitors. *Molecules* 2022;27:6797. <https://doi.org/10.3390/molecules27206797>.
- Jallouli R, Othman H, Amara S *et al.* The galactolipase activity of *Fusarium solani* (phospho) lipase. *Biochim Biophys Acta* 2015;1851:282–9. <https://doi.org/10.1016/j.bbali.2014.12.010>.
- Kato S, Motoyama T, Futamura Y *et al.* Biosynthetic gene cluster identification and biological activity of lucilactaene from *Fusarium* sp. RK97–94. *Biosci Biotechnol Biochem* 2020;84:1303–7. <https://doi.org/10.1080/09168451.2020.1725419>.
- Katoh K, Standley DM. MAFFT multiple sequence alignment software version 7: improvements in performance and usability. *Mol Biol Evol* 2013;30:772–80. <https://doi.org/10.1093/molbev/mst010>.
- Klomchit A, Calderin JD, Jaidee W *et al.* Naphthoquinones from *Neocosmospora* sp.—antibiotic activity against *Acidovorax citrulli*, the causative agent of bacterial fruit blotch in watermelon and melon. *J Fungi* 2021;7:370. <https://doi.org/10.3390/jof7050370>.
- Kolmogorov M, Yuan J, Lin Y *et al.* Assembly of long, error-prone reads using repeat graphs. *Nat Biotechnol* 2019;37:540–6. <https://doi.org/10.1038/s41587-019-0072-8>.
- Lee HS, Phat C, Nam WS *et al.* Optimization of culture conditions of *Fusarium solani* for the production of neoN-methylsalsalvamide. *Biosci Biotechnol Biochem* 2014;78:1421–7. <https://doi.org/10.1080/09168451.2014.921554>.
- Li H. Minimap2: pairwise alignment for nucleotide sequences. *Bioinformatics* 2018;34:3094–100. <https://doi.org/10.1093/bioinformatics/bty191>.
- Liu H, Bao X. Characterization of a chitosanase from *Fusarium solani* and its expression in an industrial strain of *Saccharomyces cerevisiae*. *Wei Sheng Wu Xue Bao* 2009;49:1607–12.
- Liu YJ, Whelen S, Hall BD. Phylogenetic relationships among ascomycetes: evidence from an RNA polymerase II subunit. *Mol Biol Evol* 1999;16:1799–808. <https://doi.org/10.1093/oxfordjournals.molbev.a026092>.

- Lombard L, van der Merwe NA, Groenewald JZ *et al.* Generic concepts in *Nectriaceae*. *Stud Mycol* 2015;80:189–245. <https://doi.org/10.1016/j.simyco.2014.12.002>.
- Longhi S, Nicolas A, Jelsch C *et al.* Structure-function studies on cutinase, a small lipolytic enzyme with a water accessible active site. In: *Protein Engineering For Industrial Biotechnology*. London: CRC Press, 2000, 91–130.
- Mannesse MLM, Cox RC, Koops BC *et al.* Cutinase from *Fusarium solani* pisi hydrolyzing triglyceride analogs. Effect of acyl chain length and position in the substrate molecule on activity and enantioselectivity. *Biochemistry* 1995;34:6400–7. <https://doi.org/10.1021/bi00019a020>.
- Manni M, Berkeley MR, Seppey M *et al.* BUSCO update: novel and streamlined workflows along with broader and deeper phylogenetic coverage for scoring of eukaryotic, prokaryotic, and viral genomes. *Mol Biol Evol* 2021;38:4647–54. <https://doi.org/10.1093/molbev/mab199>.
- Miller MA, Pfeiffer W, Schwartz T. The CIPRES science gateway: enabling high-impact science for phylogenetics researchers with limited resources. *ACM International Conference Proceeding Series*. New York, NY, United States, 2012.
- Nomila Merlin J, Nimal Christhudas IVS, Praveen Kumar P *et al.* Optimization of growth and bioactive metabolite production: *Fusarium solani*. *Asian J Pharm Clin Res* 2013;6:98–103.
- Norphanphoun C, Raspé O, Jeewon R, *et al.*, Morphological and phylogenetic characterisation of novel cytospora species associated with mangroves. *MycKeys* 2018;28:93–120. <https://doi.org/10.3897/mycokeys.38.28011>.
- O'Donnell K, Al-Hatmi AMS, Aoki T *et al.* No to *Neocosmospora*: phylogenomic and practical reasons for continued inclusion of the *Fusarium solani* species complex in the genus *Fusarium*. *mSphere* 2020;5:e00810–20. <https://doi.org/10.1128/mSphere.00810-20>.
- O'Donnell K. Molecular phylogeny of the *Nectria haematococca-Fusarium solani* species complex. *Mycologia* 2000;92:919. <https://doi.org/10.2307/3761588>.
- Palmer JM, Stajich J. Funannotate v1. 8.1: eukaryotic genome annotation. *Zenodo* 2020;4054262. <https://doi.org/10.5281/zenodo.28> (28 September 2020, date last accessed).
- Pfenning L. A new species of *Neocosmospora* from Brazil. *Sydowia* 1995;47:65–69.
- Rathna J, Yazhini KB, Ajilda AAK *et al.* Production of naphthoquinones and phenolics by a novel isolate *Fusarium solani* PSC-R of Palk Bay and their industrial applications. *Bioresour Technol* 2016;213:289–98. <https://doi.org/10.1016/j.biortech.2016.04.050>.
- Rossmann AY, Samuels GJ, Rogerson CT *et al.* Genera of *Bionectriaceae*, *Hypocreaceae* and *Nectriaceae* (Hypocreales, Ascomycetes). *Stud Mycol* 42 1999;4:1–248.
- Sandoval-Denis M, Guarnaccia V, Polizzi G *et al.* Symptomatic citrus trees reveal a new pathogenic lineage in *Fusarium* and two new *Neocosmospora* species. *Persoonia* 2018;40:1–25. <https://doi.org/10.3767/persoonia.2018.40.01>.
- Sandoval-Denis M, Lombard L, Crous PW. Back to the roots: a reappraisal of *Neocosmospora*. *Persoonia* 2019;43:90–185. <https://doi.org/10.3767/persoonia.2019.43.04>.
- Shahid H, Cai T, Wang Y *et al.* Duclauxin derivatives from fungi and their biological activities. *Front Microbiol* 2021;12:766440. <https://doi.org/10.3389/fmicb.2021.766440>.
- Smith EF. Wilt disease of cotton, watermelon and cowpea (*Neocosmospora* nov. gen.). *US Dep Agric Div Veg Physiol Pathol Bull* 1899;17:1–54.
- SPSS Inc. *SPSS for windows, version 16.0*. Chicago: SPSS Inc, 2007.
- Studt L, Wiemann P, Kleigrewe K *et al.* Biosynthesis of fusarubins accounts for pigmentation of *Fusarium fujikuroi* perithecia. *Appl Environ Microb* 2012;78:4468–80. <https://doi.org/10.1128/AEM.00823-12>.
- Styers TJ, Kekec A, Rodriguez R *et al.* Synthesis of Sansalvamide derivatives and their cytotoxicity in the MSS colon cancer cell line HT-29. *Bioorg Med Chem* 2006;14:5625–31. <https://doi.org/10.1016/j.bmc.2006.04.031>.
- Takemoto K, Kamisuki S, Chia PT *et al.* Bioactive dihydronaphthoquinone derivatives from *Fusarium solani*. *J Nat Prod* 2014;77:1992–6. <https://doi.org/10.1021/np500175j>.
- Tamizi A-A, Mat-Amin N, Weaver JA *et al.* Genome sequencing and analysis of *Trichoderma* (Hypocreaceae) isolates exhibiting antagonistic activity against the papaya dieback pathogen, *Erwinia mallo-tivora*. *J Fungi* 2022;8:246. <https://doi.org/10.3390/jof8030246>.
- Vaser R, Sović I, Nagarajan N *et al.* Fast and accurate de novo genome assembly from long uncorrected reads. *Genome Res* 2017;27:737–46. <https://doi.org/10.1101/gr.214270.116>.
- Vilgalys R, Hester M. Rapid genetic identification and mapping of enzymatically amplified ribosomal DNA from several *Cryptococcus* species. *J Bacteriol* 1990;172:4238–46. <https://doi.org/10.1128/jb.172.8.4238-4246.1990>.
- White TJ, Bruns T, Lee S *et al.* Amplification and direct sequencing of fungal ribosomal rna genes for phylogenetics. In: *PCR Protocols*. Cambridge, Massachusetts, United States: Academic Press, Inc., 1990.
- Wu YR, Nian DL. Production optimization and molecular structure characterization of a newly isolated novel laccase from *Fusarium solani* MAS2, an anthracene-degrading fungus. *Int Biodeterior Biodegradation* 2014;86:382–89. <https://doi.org/10.1016/j.ibiod.2013.10.015>.
- Zeng Z, Zhuang W. Eight new combinations of Bionectriaceae and Nectriaceae. *Mycosystem* 2017;36:278–81.